SEC−MALLS and SANS Studies Applied to Solution Behavior of Linear α-Glucans

Philippe Roger,* Monique A. V. Axelos, and Paul Colonna

Institut National de la Recherche Agronomique, rue de la Géraudière, BP 71627, 44316 Nantes Cedex 03, France

Received August 4, 1999; Revised Manuscript Received January 19, 2000

ABSTRACT: Both size-exclusion chromatography coupled on-line with multiangle-laser-light-scattering (SEC−MALLS) and small-angle neutron scattering (SANS) demonstrate that linear α-glucan chains adopt the conformation of random coils with a higher dimension in alkaline conditions than in water. For amylose, the mass per unit length, $M_L \sim 410$ g/mol/nm, obtained from the SEC−MALLS results, shows that the α(1,4)-glucan chain has an overall flexible character in H_2O. An insignificant difference is obtained by SANS using KOD as solvent, but when D_2O is used, M_L decreases with the molar mass. This effect is explained by a decrease in solvent quality. Then, when the radius of gyration vs the molar mass and the logarithm of the molar mass vs the elution volume relationships are considered, it is found that pullulans can be used to replace the linear amylose standards for chromatographic calibration purposes in 0.1 M KOH; the same cannot be done using water as solvent. On the contrary, the hydrodynamic radius vs elution volume calibration curve is found to be independent of the solvent and the polymer used.

Introduction

Polysaccharide macromolecular characterization is a field of interest due to major uses of polysaccharides in food industries. Polysaccharides are used for their functional properties (gelation, thickening, ...),[1] which are related to their macromolecular features, i.e., molar masses and volume occupied by the polymer chain in solution. Furthermore, liquids used in food industries are strictly water-based, which underlines the interest in obtaining the macromolecular features in this ubiquitous solvent. The availability of monodisperse water-soluble polymer standards has been the bottleneck, until recently, for all studies devoted to macromolecular features. Pioneering works were based upon chromatographic techniques: molar masses were first obtained with respect to a calibration curve built using monodisperse polymer standards. Now with the development of multidetection techniques, there is no need of this type of calibration curve for molar masses determination as absolute determination is directly obtained.

However, monodisperse polymer standards are still used to calibrate light-scattering detectors and to determine interdetector delay volume. There have been recently published results about this subject but dealing with organic solvents.[2,3]

These monodisperse polymer standards are reference materials when studying the degree of branching of a polymer when multidetection is used. By SEC−MALLS the two possibilities are to follow either the branching ratio of the radii of gyration, $g_M = R_{Gbranched}/R_{Glinear}$ at the same molar mass, M, or the branching ratio of the molar masses, $g_V = M_{linear}/M_{branched}$ at the same elution volume, V_e. Whatever the procedure, accurate R_G vs M and M vs elution volume calibration curves have to be obtained for the equivalent linear standards.

The aim of this work is to consider how these equations can be applied to two linear α-glucans: amylose and pullulan. Amylose is a 1→4 α-D-glucan whereas pullulan is based upon the repetition of →6-α-D-Glcp-1→4-α-D-Glcpl-1→4-α-D-Glcp-1→.

Whereas pullulan samples with a rather narrow distribution of molecular mass are commercially available, this is not the case for amylose. That is the main reason for us to undertake the synthesis of amylose fractions. Furthermore, the use of de novo amylose samples prepared by an enzymatic method will overcome difficulties encountered with amyloses extracted from starch. The major problem is that the extracted amylose is polluted by amylopectin unless an ultracentrifugation treatment in alkaline solution is applied. Then a small amount of the high molar mass amylopectin will definitely lead to erroneous R_G vs M and M vs elution volume calibration curves.[4,5]

The macromolecular features of amylose and pullulan will be obtained by SEC−MALLS. This method presents several advantages vs static LS alone. First, it is faster (it takes only the time of the on-line fractionation process, i.e., 30 min in our case), and only one stock solution has to be studied (there is no need of several dilutions). If systematic errors such as the calibration of the MALLS and the refractometer detectors, the delay volume between those two instruments, and the normalization of the photodiodes of the MALLS instrument are reduced, then the SEC−MALLS method can be considered to be as accurate as the static LS for the evaluation of absolute values of molar masses and radii of gyration. The uncertainty is considered customarily to be 3−5% for M_w and 5−10% for R_{gz}. However the main advantage of using SEC−MALLS is the fact that the complete molecular weight distribution can be obtained. That allowed us to select among all the synthesis that we have undertaken the samples with the narrower molecular weight distribution. In our previous paper[6] dealing with scaling laws of amylose, the polydispersity of our samples were unknown.

Macromolecular features gained by SEC−MALLS carried out in H_2O and 0.1 M KOH will be compared to the values obtained by SANS using D_2O and 0.1 M KOD as solvents.

* To whom correspondence should be addressed. Telephone: (33) (0) 2 40675148. Fax: (33) (0) 2 40675167.

10.1021/ma991302s CCC: $19.00
Published on Web 03/09/2000

Table 1. Conditions for the Enzymatic Synthesis of the Different Amyloses

amylose synthesis	starter mg)	DG1P (g)	incubation time (h)	M^a (g/mol)
S1	0.5	3	20.5	2.2×10^6
S2	0.5	2	14.75	1.6×10^6
S3	0.5	2	8.0	1.0×10^6
S4	0.5	2	5.5	8.3×10^5
S5	1.0	2	8.5	7.7×10^5
S6	1.5	2	8.5	4.1×10^5
S7	1.0	1	2.25	2.0×10^5
S8	1.5	2	2.5	1.9×10^5
S9	1.0	2	4.25	9.0×10^4
S10	4.0	1	0.5	4.6×10^4
S11	30	2	1.5	2.0×10^4
S12	56	2.1	1.0	1.2×10^4
S13	18	0.5	0.75	7.9×10^3

[a] As obtained from phosphate analysis (see text).

Experimental Section

The amylose fractions were synthesized by using maltohexaose and glucose 1-phosphate (dipotassium salt) (DG1P) both obtained from Sigma (St. Louis, MO). Potatoes (Nicola cultivar) were used rapidly after harvesting.

The potato phosphorylase was purified according to different protocols.[7−9] Potatoes (2.5 kg) were peeled, sliced, and mechanically liquidized. The crude extract was poured in a beaker cooled with ice-cold water, containing 250 mL of a solution A (100 mM of Tris buffer (pH 7.2), 0.2 M NaCl and 0.02% sodium azide) to which 30 mM of sulfite sodium (Na_2SO_3) was added. It was kept at 4 °C until filtration on Büchman beaker using Whatman filters (11 cm, GF/A). The extract was then centrifuged (650*g*, 10 min, 4 °C), and the supernatant was recovered and then heated at 55.5 °C for 45 min to destroy α-amylase activity and finally centrifuged (650*g*, 10 min, 4 °C). This last supernatant was made up to 180 g/L ammonium sulfate, and after 1 h in ice cold water, the precipitate was removed by centrifugation (1400*g*, 5 min, 4 °C). The ammonium sulfate concentration was adjusted to a density of 1.150 at 15 °C to precipitate phosphorylase. After one night at 4 °C and centrifugation (2500*g*, 5 min, 4 °C), the precipitates containing phosphorylase were dissolved in the minimum volume of solution A and completed to 100 mL to get a crude enzymatic preparation. At this step, phosphorylase activity was tested by mixing 250 μL of a solution (10 mL) containing 1 mg of maltohexaose, 50 mg of DG1P in a citrate buffer (pH = 6.2) and 250 μL of the enzymatic solution containing phosphorylase. A few drops of I_2/IK was then added: phosphorylase activity was detected when a blue color occurred. To separate phosphorylase from other enzymes, the crude enzymatic preparation (15 mL) was injected onto a column containing 525 mL of a Sephacryl S-300 HR gel (Pharmacia) eluted with A at a flow rate of 100 mL/h. Fractions were collected every 5 min. Fractions (generally four tubes) containing phosphorylase activity were recovered after 90 min for 20 min: they were pooled and stored at 4 °C before use as such in the reaction of polymerization (phosphorylase solution). Protein concentration was checked by the method of Lowry.[10]

Phosphorylase-Catalyzed Amylose Synthesis. A solution (10 mL) of glucose 1-phosphate dissolved in water, adjusted to pH 6.2 with 2 M acetic acid and mixed to 0.1 M citrate buffer pH 6.2 (4 mL), a solution (1 mL) of maltohexaose dissolved in water, and the phosphorylase solution (20 mL), prepared as above, were mixed, completed to 100 mL with water, and incubated at 37 °C until the desired molecular weight was reached. Quantities of maltohexaose and glucose 1-phosphate and the incubation times used are shown in Table 1. Every 15 min, an aliquot was removed for immediate phosphate analysis. At the end of the incubation period, proteins in the remaining solution were denatured by heating to 95 °C for 30−40 min under vigorously bubbling nitrogen. Precipitated proteins were immediately removed by filtration (12.5 cm, 113^V, Whatman), and amylose was isolated by one of the following two methods depending on chain length. For chain lengths >500 glucosyl units, the amylose solution was cooled to 70 °C, 1-butanol added to 10% v/v, the mixture slowly cooled, and the resulting precipitate collected, washed with ethanol (4×) and diethyl ether (2×), and air-dried. For chain lengths of <500 glucosyl units, the hot amylose solution was mixed with four volumes of ethanol and the precipitate collected by filtration as above.

Phosphate Analysis. Molar masses of synthesized amyloses can be first approximated by phosphate analysis[11] of incubation mixtures. As one molecule of phosphate is produced for each glucose unit added to a synthetic amylose chain, phosphate analysis can be used to derive amylose molar masses by assuming a monodisperse population of chains and by assuming that all the maltohexaose moieties are used as primers. The reaction was stopped when the desired molecular weight was reached.

Pullulan Standards. A set of nine pullulan standards P-82 (Showa Denko K. K.; Tokyo, Japan) was also used.

Sample Preparation for SEC−MALLS: For the preparation of amylose solutions in 0.1 M KOH, amylose powders were dispersed in 1 M KOH, gently stirred overnight at 4 °C, and then diluted to 0.1 M KOH.

For water solutions, synthetic amylose powders were dispersed in boiling water over 5−30 min until clarity is obtained. Amylose solutions were then cooled to room temperature.

All samples were filtered directly into the autosampler cell through Durapore HV (0.45 μm) without effects on amylose concentrations, which were in the range 1−5 g·L^{-1}. Concentrations were checked before injection by the sulfuric acid−orcinol colorimetric method,[12] and the amylose samples recovery calculated from the area of the RI profile was always greater than 95%.

Size-Exclusion Chromatography−Multiangle Laser-Light Scattering. The SEC−MALLS equipment was the same as the one described previously[4] except that a Waters 590 programmable HPLC pump (Waters, Milford, MA) and a Waters 717 autosampler were used. The packing of the columns used (Shodex OHpak KB-800 series (300 mm × 8 mm) (Showa Denko K. K., Tokyo, Japan)) is a strong poly(hydroxymethyl methacrylate) gel designed for the separation of polysaccharides. They were shown to work for years even under alkaline conditions at high pH values. They were connected in the order KB-806, KB-805, and KB-804 with an estimated exclusion limit given by the furnisher using poly(ethylene glycol) of 2×10^7, 4×10^6 and 4×10^5 g·mol^{-1} respectively. Columns were maintained at 40 °C using a Crococil temperature control (Cluzeau, Bordeaux, France).

The MALLS detector, a Dawn DSP−F fitted with a K5 flow cell and a He−Ne laser, ($\lambda = 632.8$ nm), from Wyatt Technology Corp. (Santa Barbara, CA) was installed on-line between the columns and the refractometer (ERC-7510, Erma Optical Works Ltd., Tokyo, Japan). Number-average molar mass ($\bar{M}_n$), weight-average molar mass ($\bar{M}_w$), polydispersity index $\bar{M}_w/\bar{M}_n$ and w- and *z*-average root-mean-square (rms) radii of gyration in nm were established with ASTRA software (version 1.4 for Macintosh) by using the following summations taken over one peak.

Number-average molar mass:

$$\bar{M}_n = \frac{\sum c_i}{\sum \frac{c_i}{M_i}} \quad (1)$$

Weight-average molar mass:

$$\bar{M}_w = \frac{\sum (c_i M_i)}{\sum c_i} \quad (2)$$

Weight-average radius of gyration:

$$\bar{R}_{gw} = \langle r^2 \rangle_w = \frac{\sum (c_i \langle r^2 \rangle_i)}{\sum c_i} \quad (3)$$

z-Average radius of gyration:

$$\bar{R}_{gz} = \langle r^2 \rangle_z = \frac{\sum (c_i M_i \langle r^2 \rangle_i)}{\sum c_i M_i} \quad (4)$$

The quantities c_i, M_i, and $\langle r^2 \rangle_i$ in the above equations are respectively the mass concentration, molar mass, and mean square radius of the ith slice. M_i and $\langle r^2 \rangle_i$ are obtained at each slice of the chromatogram peak after an extrapolation procedure detailed below.

A value of 0.146 mL·g^{-1} was employed as the refractive index increment (dn/dc) for both glucans.[13] An interdetector delay volume of 175 μL was determined by injecting BSA monomer (Sigma Chemical Co., Poole, U.K.), i.e., a purified bovine serum albumin sample with a very narrow molar mass distribution.

Extrapolation Procedure. Under our aqueous conditions, 15 angles are available in the Dawn-DSP in the range 22−158°. However, when extrapolating at zero angle using any one of the three extrapolation methods available (Debye, Zimm, Berry), it was observed that the three lowest angles (22, 29, 36°) and the three highest (144, 151, 158°) did not systematically belong to the extrapolated line (Figure 1) and increased the uncertainty in the calculated molar mass and radius of gyration averages. These uncertainties, listed later in the text, are only statistical uncertainties due to the extrapolations performed for each slice. They do not include any of the many possible systematic errors mentioned in the Introduction. These six angles were thus not used in the following to obtain better accuracy. The nine remaining angles which are in the range 44−136° still allow a good determination of molecular characteristics in the limit of the Guinier range i.e., $q\bar{R}_G < 1$, where **q** is the scattering vector defined as

$$q = (4\pi n/\lambda) \sin(\theta/2) \quad (5)$$

where θ is the scattering angle, λ the wavelength of the incident light in a vacuum, and n the index of refraction of the scattering medium.

Small-Angle Neutron Scattering. Equipment. The neutron scattering experiments were carried out with a small-angle neutron spectrometer, PACE, at the Laboratoire Léon Brillouin, C.E.-Saclay, France. The experimental scattering intensity $I(q)$ was collected using a sample detector distance $D = 1.85$ m with $\lambda = 7.5 \pm 0.5$ Å, covering a scattering vector **q** range from 1.36×10^{-2} Å^{-1} to 1.43×10^{-1} Å^{-1}) where q is given by

$$q = (4\pi/\lambda) \sin(\theta/2) \quad (6)$$

θ being the scattering angle.

Amylose samples S3, S6, S7, S10, and S13 were dispersed in 1 M KOD and diluted to 1:10 for further analysis in 0.1 M KOD at 25 °C. Amylose samples S3, S6, and S7 were dispersed in boiling D_2O and kept at 40 °C due to precipitation of amylose chains occurring in D_2O at 25 °C. Dissolving S10 and S13 in D_2O was unsuccessful. All the solutions were filtered through a 0.45 μm filter and poured into 1 mm wide quartz cells.

The raw data were corrected for scattering from the empty cell, sample thickness, transmission, and detector efficiency. The scattering was normalized to water, which was used as a standard and is in absolute units (cm^{-1}).

Method. The q range was chosen in order to obtain the persistence length, a, and the mass per unit length M_L, i.e., to be able to observe the transition between the Debye regime (where the chains behave as random coils), where $\bar{R}_G^{-1} < q < a^{-1}$, and the Porod domain (where the chains are observed as rigid rods), where $q \gg a^{-1}$.

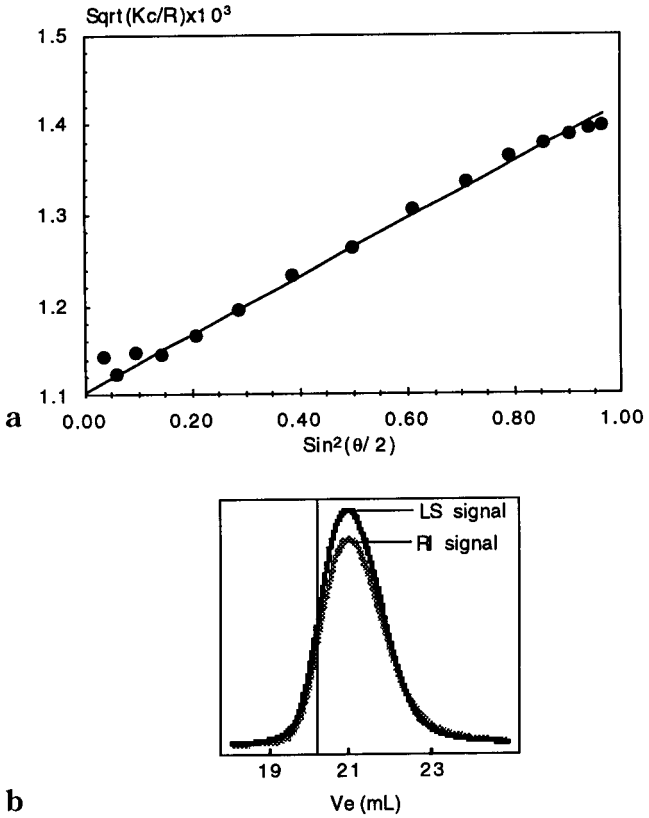

Figure 1. Berry extrapolation plot of one slice of sample S3 using KOH 0.1 M as solvent (a, top). All the available angles are shown. The chromatogram (b, bottom) indicating the position of the corresponding slice with a vertical line.

In the case of a monodisperse Gaussian chain, scattering intensity $I(q)$ is proportional to the scattering form factor, $P(u)$ (Debye equation):

$$P(u) = 2(e^{-u} + u - 1)/u^2 \quad (7)$$

with $u = q^2\bar{R}_G^2$.

This function has an asymptotic behavior in q^{-2} in the high q range. Then, if $I(q)$ is related to the molar mass M, the expression $Mq^2I(q)$ in the high q range becomes:[14]

$$\lim_{q \to \infty} Mq^2I(q) = 6M_L/a(1 - 3M_L/q^2Ma) \quad (8)$$

In the case of a cylinder of length L, the $I(q)$ function normalized to M is given at high q values[14]

$$\lim_{q \to \infty} Mq^2I(q) = \pi M_L q - 2M_L/L \quad (9)$$

and becomes in the range of high L

$$\lim_{L \to \infty} Mq^2I(q) = \pi M_L q \quad (10)$$

This equation corresponds to a line with the origin as intercept in a plot of $q^2I(q)$ vs q. It is then possible to obtain M_L from the slope.

Finally in a plot of $q^2I(q)$ vs q, usually called a Kratky plot, it is possible to visualize the transition from the coil scattering behavior (eq 7) with an asymptote parallel to the abscissa (eq 8) to the asymptotic rod scattering behavior of eq 10. The point of intersection of abscissa q^* between both abscissa is obtained from

$$\pi M_L q^* = 6M_L/a \quad (11)$$

So the persistence length can be calculated from the q^* value:

$$a = 6/\pi q^* \quad (12)$$

Results

Macromolecular Characteristics of Amylose and Pullulan Samples. A set of 13 enzymatically made amyloses was synthesized. These samples are called from S1 to S13 in the order of decreasing molar mass. The conditions of the different reactions (quantity of primer and of DG1P, incubation time, MW obtained by phosphate analysis, ...) are given in Table 1. The molar masses obtained from phosphate analysis ranged from 7.9×10^3 to 2.2×10^6 g/mol.

These samples are then characterized by using both 0.1 M KOH and water as solvent. SEC−MALLS results, i.e., the weight-average molar mass, $\bar{M}_w$, the polydispersity index, $\bar{M}_w/\bar{M}_n$, and the *z*-average radius of gyration, $\bar{R}_{Gz}$, are given in Tables 2 and 3 using 0.1 M KOH and water as solvent, respectively. The Berry extrapolation method was chosen as already suggested for narrow molecular mass distribution.[15]

In 0.1 M KOH, $\bar{M}_w$ values are in the range 1.2×10^4 to 1.2×10^6 g·mol^{-1} and $\bar{R}_{Gz}$ from 9 to 63 nm. The statistical error in $\bar{M}_w$ is less than 1% down to 5×10^4 g/mol and increases up to 5% for the lowest molar mass of 1.2×10^4 g/mol. The range of error in $\bar{R}_{Gz}$ values is broader (1−30%), and the error increases especially in the case of radii of gyration lower than 20 nm. For larger macromolecules the more pronounced angular dependencies improve the accuracy of the extrapolation with uncertainties in the range 1−5%.

For $\bar{M}_w$ below 2.4×10^5 g·mol^{-1}, dissolution was unsuccessful even in hot water. For the eight remaining samples from S1 to S8, SEC−MALLS characterization in water gives $\bar{M}_w$ ranging from 2.4×10^5 to 1.2×10^6 g·mol^{-1} and $\bar{R}_{Gz}$ from 17 to 40 nm. The statistical uncertainty is less than 1% for $\bar{M}_w$ whereas it is in the range 1−6% in the case of $\bar{R}_{Gz}$.

Results of the polydispersity indexes, $\bar{M}_w/\bar{M}_n$, do not depend on solvent type. They are very low and are not higher than 1.01 for $\bar{M}_w$ below 2.4×10^5 g·mol^{-1} and then increase up to 1.02−1.17 for $\bar{M}_w$ above 2.4×10^5 g·mol^{-1}. For the polydispersity index, the precision is in the range 2−10%.

For the same batch sample, there is nearly no difference between $\bar{M}_w$ obtained in 0.1 M KOH and water as solvent: no degradation of amylose has occurred in those conditions. But $\bar{M}_w$ obtained using SEC−MALLS differs sometimes significantly from the molar mass as determined by phosphate analysis, this last analysis has to be considered only as an indicative one which stops the enzymatic reaction and provides only an approximate value of $\bar{M}_w$.

Molar Mass Dependence of $\bar{R}_G$. For amylose samples radius of gyration values in 0.1 M KOH are systematically higher than those in water. The expansion of amylose in KOH is clearly seen in Figure 2 where the double logarithm of $\bar{R}_{Gw}$ vs $\bar{M}_w$ is plotted. $\bar{R}_{Gw}$ is used instead of $\bar{R}_{Gz}$ to take into account the increase in polydispersity index for the higher $\bar{M}_w$. The exponent ν in the power law

$$\bar{R}_{Gw} = K\bar{M}_w^{\nu} \quad (13)$$

gives evidence in solvent quality: the values are 0.62 ± 0.06 and 0.52 ± 0.02 respectively in KOH and water taking into account the statistical uncertainties in each number. The value obtained in KOH 0.1 M is slightly higher but not significantly different than the theoretical value calculated for a random coil under a good solvent condition which takes the value of 0.6 at the asymptotic limit of the excluded volume effect in Flory's theory[16,17] and 0.588 in the renormalization calculation.[18] The coefficient obtained in water is close to the value 0.5 expected under the Θ-conditions where the dimension of the chain is unperturbed by the solvent. The expansion of the radius of gyration in KOH 0.1 M can be characterized by the expansion factor α_s, $\alpha_s = \bar{R}_{Gz(KOH)}/\bar{R}_{Gz(H_2O)}$, which is found to increase with $\bar{M}_w$− from 1.4 to 1.6 in the molar mass range 2×10^5 to 1.2×10^6 g·mol^{-1}.

Pullulan was studied in the same way by SEC−MALLS in the $\bar{M}_w$ range 6×10^3 to 1.3×10^6 g·mol^{-1}.

Table 2. Macromolecular Characteristics of Synthetic Amyloses Using 0.1 M KOH as Solvent Determined by SEC−MALLS

amylose synthesis	$\bar{M}_w$ (g/mol)	$\bar{M}_w/\bar{M}_n$	$\bar{R}_{Gz}$ (nm)
S1	1.2×10^6	1.17	63.2
S2	1.1×10^6	1.09	58.5
S3	7.7×10^5	1.03	47.9
S4	5.5×10^5	1.11	40.5
S5	4.8×10^5	1.10	37.4
S6	4.1×10^5	1.00	32.1
S7	2.9×10^5	1.01	25.6
S8	2.3×10^5	1.00	23.4
S9	8.7×10^4	1.01	11.6
S10	5.0×10^4	1.00	9.0
S11	2.4×10^4	1.00	nd
S12	1.7×10^4	1.01	nd
S13	1.2×10^4	1.01	nd

Table 3. Macromolecular Characteristics of Synthetic Amyloses Using Water as Solvent Determined by SEC−MALLS

amylose synthesis	$\bar{M}_w$ (g/mol)	$\bar{M}_w/\bar{M}_n$	$\bar{R}_{Gz}$ (nm)
S1	1.2×10^6	1.15	40.0
S2	1.1×10^6	1.11	38.0
S3	8.0×10^5	1.03	30.5
S4	5.9×10^5	1.09	27.7
S5	5.2×10^5	1.11	25.5
S6	4.3×10^5	1.00	22.5
S7	3.1×10^5	1.01	18.9
S8	2.4×10^5	1.00	16.9

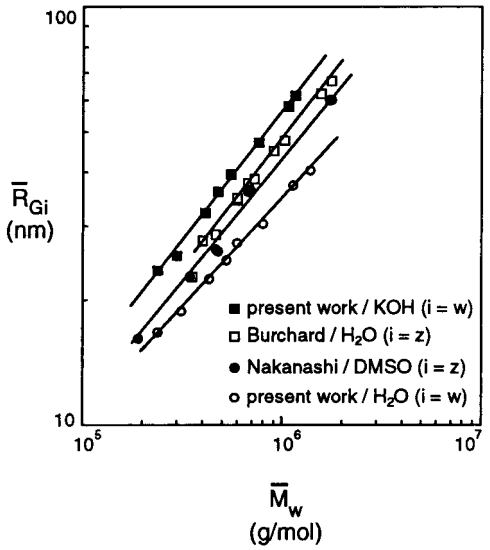

Figure 2. The log−log plots of the $\bar{M}_w$ dependence of $\bar{R}_{Gw}$ of amylose fractions in H_2O and 0.1 M KOH (present results) and log−log plots of the $\bar{M}_w$ dependence of $\bar{R}_{Gz}$ of amylose fractions in DMSO (Nakanishi et al., 1993) and water (Burchard, 1963).

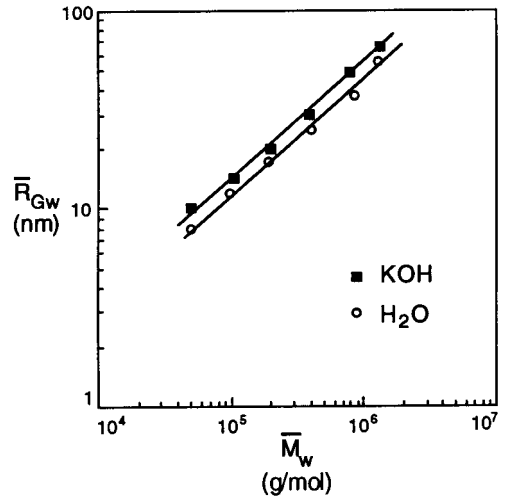

Figure 3. The log−log plots of the $\bar{M}_w$ dependence of $\bar{R}_{G_w}$ of pullulans in H_2O and 0.1 M KOH.

The statistical uncertainties in $\bar{M}_w$ and $\bar{R}_{Gz}$ are in the same range as for amylose. Figure 3 shows that an expansion of the radius of gyration is also obtained for pullulan in KOH compared to water. Moreover, if a Zimm extrapolation is used, $\bar{R}_{Gz}$ and $\bar{M}_w$ values in water (Table 4) verify the relationship established using classical light scattering by others,[19] which assess our experimental conditions.

For pullulans, the difference in radii between the two solvents is less than that for amyloses with a constant expansion factor $\alpha_s \sim 1.2$. Then by using the statistical uncertainties to each $\bar{R}_{Gw}$ and $\bar{M}_w$ values, the ν exponents obtained in eq 14 are not significantly different (0.62 ± 0.06 in KOH and 0.58 ± 0.07 in water), indicating that pullulan adopts nearly the same conformation in both solvents, i.e., a random coil fully expanded due to the excluded-volume effect.

When considering both polymers in the same solvent, the scaling laws (eq 13) obtained for amylose and pullulan in KOH are identical, meaning that those two glucans behave in the same way in this solvent. The effectiveness of this medium as a solvent for glucans is undoubtedly due to ionization of hydroxyl groups with pK_a values not too much higher than 12. The scaling exponent obtained ($\nu = 0.62$) characterizing a modest chain expansion accompanying this ionization is presumably due to the relatively high ionic strength of the ionizing medium.

In water, the radii of gyration differ significantly with larger dimensions for pullulan than for amylose and differences increasing from 14 to 27% when molar mass shifts from 2×10^5 to 1.2×10^6 g·mol^{-1}. That can be easily explained considering that the random coil conformation is adopted by both glucan and that water at 25 °C is a good solvent for pullulan whereas it is a Θ-solvent for amylose.

Our $\bar{R}_{Gw}$ and $\bar{M}_w$ results on amylose are then compared on the same graph (Figure 2) to the $\bar{R}_{Gz}$ and $\bar{M}_w$ data obtained for synthetic amylose in water[20] and in DMSO.[15] It is possible to compare those curves because the difference in $\bar{R}_{Gz}$ and $\bar{R}_{Gw}$ data is indistinguishable on that kind of log−log plot. DMSO is considered to be a good solvent for starch polysaccharides. These authors have effectively found a coefficient of 0.6 in the relation using synthetic amylose fractions. On the log−log plot of $\bar{R}_{Gz}$ vs $\bar{M}_w$, the line corresponding to DMSO is well below the line corresponding to Burchard's results and above the line corresponding to our results, but it seems unlikely that amylose would adopt a higher dimension in water which has been shown here to be a Θ-solvent than in DMSO which is a good solvent.

The log *M* vs Elution Volume Equations. The log M vs V_e curves for amylose (Figure 4) show an increase in elution volume using water as solvent as compared to 0.1 M KOH as solvent for the same amylose $\bar{M}_w$. If the pure exclusion effect is assumed to be responsible for the chromatographic process, then the elution volume is inversely proportional to the hydrodynamic size, and the difference between the two curves means that amylose has a higher hydrodynamic size in KOH than in water. Considering a fixed elution volume in the range from 20.5 to 23.5 mL, the ratio between the two respective molar masses M_{KOH}/M_{H_2O} decreases from 1.58 to 1.36. The two log K vs V_e curves for pullulan in those two solvents are more similar than in the case of amylose (Figure 5). Considering the same elution volume range, the ratio M_{KOH}/M_{H_2O} decreases to 1.11−1.19. It means in both cases that the respective α-glucan polymer chains are more dense in water than under alkaline conditions for the same volume occupied or, in other terms, that the polysaccharides chains are more expanded in 0.1 M KOH than in water.

Considering now the difference of log M vs V_e behaviors between pullulan and amylose in the same solvent, the ratio M_{PUL}/M_{AMY} decreases from 1.19 to 1.06 with the elution volume using 0.1 M KOH as solvent whereas it increases from 0.86 to 0.93 using H_2O in the same elution volume range as previously, i.e., from 20.5 to 23.5 mL. So in water, amylose is found to be less expanded than pullulan. This result has been already pointed out by others[21] who used SEC−LALLS (low-angle laser-light scattering) and neutral aqueous buffer as the eluent. In 0.1 M KOH, the inverse trend is found; i.e., amylose is more expanded than pullulan.

The differences between the log M vs V_e curves lead to the same conclusions and interpretations as those drawn from the $\bar{R}_G$ vs $\bar{M}_w$ relationships; i.e., the difference of size between 0.1 M KOH and H_2O is more important for amylose than for pullulan chains.

From those two studies of $\bar{R}_G$ vs $\bar{M}_w$ and log M vs V_e relationships, it can be concluded that if pullulan can be used instead of amylose as standards in 0.1 M KOH to obtain roughly similar calibration equations, which cannot be done if water is used as the eluent.

Small-Angle Neutron Scattering. The macromolecular features were obtained by SANS in D_2O at 40 °C and KOD 0.1 M at 25 °C. Concentrations used for the SANS experiments are below the overlapping concentration c^* (Table 5) which is calculated from

$$c^* = 3\bar{M}_w/4\pi\bar{R}_G{}^3 \qquad (14)$$

where $\bar{R}_G$ and $\bar{M}_w$ are the values obtained experimentally in the aqueous solvents KOH and H_2O.

Kratky plots were not used to extract a and M_L values as the transition between the flexible behavior and the rigid rod domain was not clear specially for molar mass below 4×10^5 g/mol. We prefer to use the log $I(q)$ vs log q curves, where the transition between a Gaussian behavior with a slope ~ -2 in the range of low q values to a rigid structure (slope ~ -1) in the range of high q values, as is theoretically expected from eqs 8 and 10 where both sides of the equations have to be multiplied by q^{-2}, is more easily observed (Figure 6a). That kind

Table 4. Manufacturer's and SEC−MALLS Macromolecular Characteristics of P82 Pullulan Standards[a]

	manufacturer		0.1 M KOH			H_2O		
pullulan	$\bar{M}_w$ (g/mol)	$\bar{M}_w/\bar{M}_n$	$\bar{M}_w$ (g/mol)	$\bar{M}_w/\bar{M}_n$	$\bar{R}_{Gz}$ (nm)	$\bar{M}_w$ (g/mol)	$\bar{M}_w/\bar{M}_n$	$\bar{R}_{Gz}$ (nm)
P1600	1.7×10^6	1.19	1.3×10^6	1.03	67.4	1.3×10^6	1.06	57.5
P800	8.5×10^5	1.14	8.0×10^5	1.07	50.9	8.5×10^5	1.05	39.0
P400	3.8×10^5	1.12	3.9×10^5	1.03	30.4	4.0×10^5	1.03	25.5
P200	1.9×10^5	1.13	2.0×10^5	1.03	20.4	1.9×10^5	1.04	17.5
P100	1.0×10^5	1.10	1.1×10^5	1.02	14.8	9.7×10^4	1.03	12.6
P50	4.8×10^4	1.09	4.9×10^4	1.01	10.0	5.0×10^4	1.02	8.0
P20	2.4×10^4	1.07	2.2×10^4	1.01	8.0	2.2×10^4	1.01	nd
P10	1.2×10^4	1.06	1.3×10^4	1.01	nd	1.3×10^4	1.03	nd
P5	5.8×10^3	1.07	6.2×10^3	1.01	nd	6.0×10^3	1.01	nd

[a] The $\bar{R}_{Gz}$ values shown in this table are obtained using a Zimm extrapolation

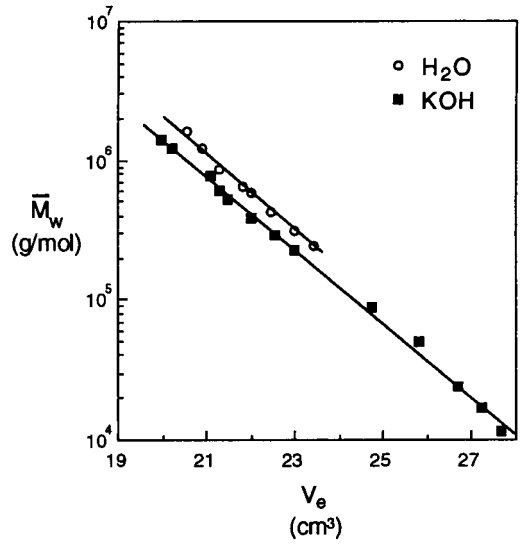

Figure 4. The log−ln plots of the elution volume, V_e, dependence of $\bar{M}_w$ of amylose fractions in H_2O and 0.1 M KOH.

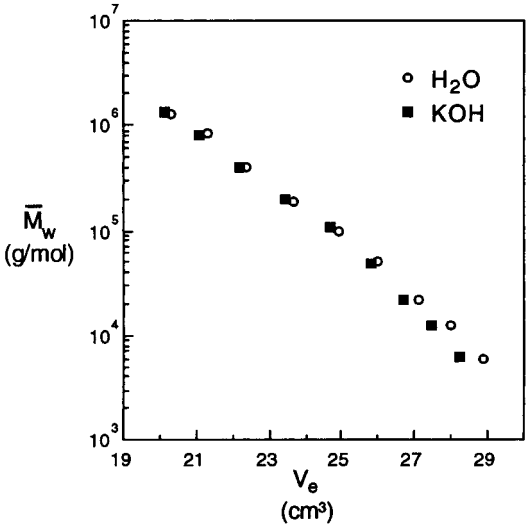

Figure 5. The log−ln plots of the elution volume, V_e, dependence of $\bar{M}_w$ of pullulans in H_2O and 0.1 M KOH.

of plot was used to visualize the change in slopes of log $I(q)$ vs log q for these two domains occurring for a q^* value which corresponds to a persistence length, a, calculated from eq 12.

Surprisingly, the values of the persistence lengths, a, are higher in KOD, with $a = 4.2$ nm for S3, S6, S7, and S10 and 55 nm for S13, than in D_2O, with $a = 1.9$, 2.8, and 3.2 nm, respectively for S3, S6, and S7.

The mass per unit length M_L is deduced from the plot of $I(q)q$ vs q (Figure 6b) which in the high q range should

Table 5. Experimental Conditions and Macromolecular Characteristics Obtained by SANS Using D_2O or KOD as Solvent for Synthetic Amyloses

	c^*(g/L)		c (g/L)		a (nm)		M_L[a] (g/mol/nm)	
amylose synthesis	KOH	H_2O	KOD	D_2O	KOD	D_2O	KOD	D_2O
S3	2.9	11	2.5	2.5	4.2	1.9	470	440
S6	4.4	14	5.3	5.3	4.2	2.8	440	510
S7	6.8	17	11	10	4.2	3.2	430	570
S10	27	nd	20	nd	4.2	nd	490	nd
S13	nd	nd	31	nd	55	nd	220	nd

[a] Obtained from the constant value on the plot of $I(q)q$ vs q in the high-q range

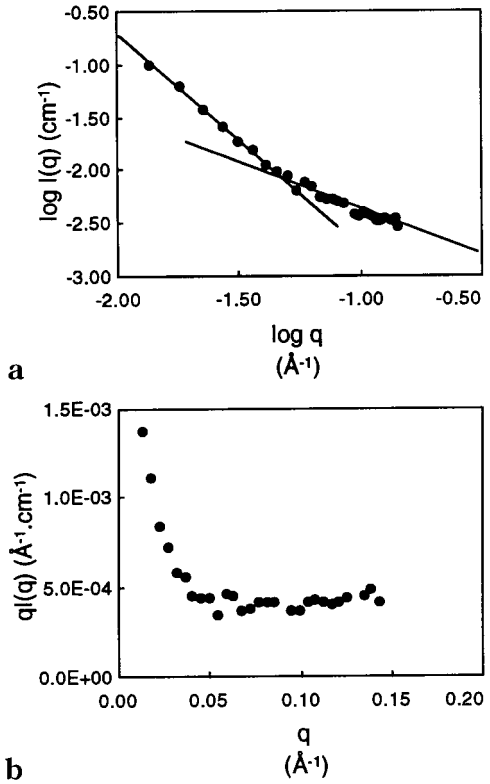

Figure 6. SANS plots of sample S6 in 0.1 M KOD (a, top) log $I(q)$ vs log q and (b, bottom) $qI(q)$ vs q.

be constant with the value πM_L (eq 10 where both sides of the equation have to be multiplied by q^{-1}). By using that kind of plot, M_L values are 470, 440, 430, 490, and 220 g/mol/nm respectively for S3, S6, S7, S10, and S13 in KOD and take the M_L values 440, 510, and 570 g/mol/nm respectively for S3, S6 and S7 in D_2O.

The unlikely values of a and M_L obtained for S13 may be explained because of the too low molar mass (1.2×10^4 g/mol) of the sample. In fact eqs 8 and 10 are only

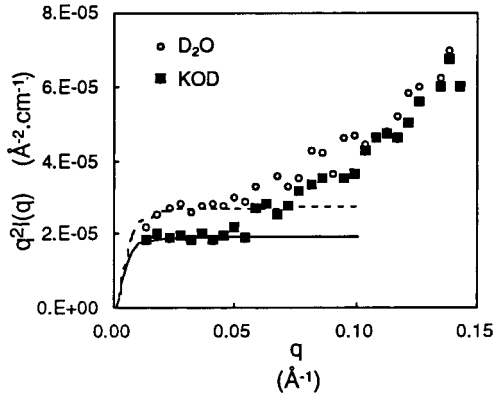

Figure 7. $q^2I(q)$ vs q plots of sample S6 in D_2O and in 0.1 M KOD. The curves represent the fit of the experimental results using the Debye equation in D_2O (full line) and 0.1 M KOD (broken line). See text for details.

valid in the limit of large n and L values. It has been stated[14] that the asymptotic behavior of eq 10 can be reached only for $L = M/M_L = 500a$, i.e., for molar masses higher than 2×10^5 g/mol if a M_L value of 450 nm^{-1} is used. From the similar results of a and M_L obtained for molar masses in the range 5×10^4 to 1×10^6 g/mol, it seems that this limit has been slightly overestimated. But it looks like it has been exceeded for a molar mass of 1.2×10^4 g/mol.

In a Kratky plot, $I(q)q^2$ vs q is a constant in the low q range (eq 8) whereas it is a line with a slope 1 in the high q range (eq 10). Differences between the two solvents are particularly appreciable on that kind of plot: the plateau in the low q range is found to be higher in D_2O than in KOD. That can be explained by a difference in $\bar{R}_G$ values in these two solvents and can be easily modeled by adjusting the value of $\bar{R}_G$ using eq 7 in order to fit the experimental $I(q)q^2$ vs q curve in the low q range. Figure 7 shows that good fits between theoretical curves and the corresponding experimental curves can be obtained. The values of $R_{G\ KOD}$, respectively 50, 32, and 25 nm for S3, S6, and S7, used to fit the experimental curve in KOD correspond well to the ones, 48, 32, and 26 nm, obtained previously in KOH by SEC−MALLS. For S3 and S6, the values of $\bar{R}_{G(D_2O)}$, respectively 36 and 26 nm, used to fit experimental curves in D_2O are higher than SEC−MALLS values which are 30.5 and 22.5 nm. Then for S7, $\bar{R}_{G(D_2O)} = \bar{R}_{G(H_2O)} = 19$ nm. For S10 and S13 in KOD, it was not possible to obtain $\bar{R}_G$ values by SANS as the plateau on the plot of $I(q)q^2$ vs q was not observed.

General Discussion

A first output of this work concerns the use of amylose and pullulan as standards in SEC. Both light scattering and SANS demonstrate that those α-glucan chains adopt the conformation of random coils with a higher dimension in KOH 0.1 M than in water. For HPSEC behaviors, absence of nonsteric exclusion effect has to be proved. Let us consider two fractions eluting at the same volume in water and in KOH. For instance, S7 in water and S8 in 0.1 M KOH elute nearly at the same volume (~23 mL), and $\bar{R}_G$ (S7/H_2O) = 18.9 nm and $\bar{R}_G$ (S8/KOH) = 23.4 nm. Hydrodynamic radii can be obtained from the structure factor $\rho = \bar{R}_G/\bar{R}_H$ which is known to be 1.5 in water and 1.78 in 0.1 M KOH, respectively, considering a random coil in a Θ solvent for the first case and a random coil in a good solvent

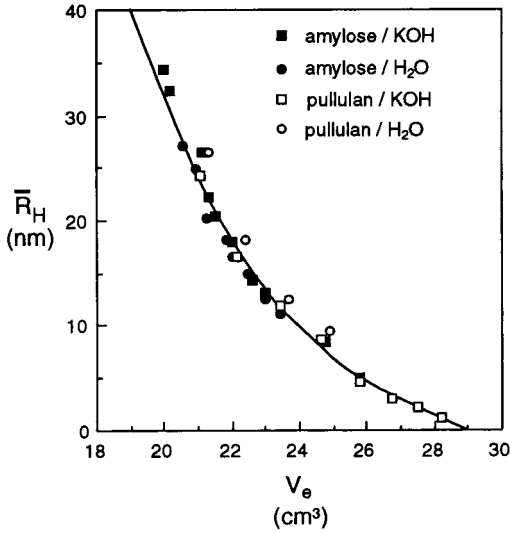

Figure 8. $\bar{R}_H$ vs V_e plots of amylose and pullulan fractions in H_2O and 0.1 M KOH.

for the second case.[22] Then $\bar{R}_H$(S7/H_2O) = 12.6 nm and $\bar{R}_H$(S8/KOH) = 13.1 nm. Hydrodynamic radii also do not differ by more than 1 nm for S5/S6 and S6/S7, respectively, in water and KOH as solvent. So fractions presenting the same elution volume in water and 0.1 M KOH have the same hydrodynamic radius: this observation means that a pure exclusion phenomenon occurs. By an extension of this approach, a plot of $\bar{R}_H$ vs elution volume (Figure 8) has been constructed using the values obtained from $\bar{R}_G$ either in water or KOH divided by the corresponding ρ factor. A master curve is obtained using a third-order polynomial equation to fit the data. This single calibration curve can be used independently of the eluent (water or KOH 0.1 M) but also independently of the α-glucan structure (pullulan or amylose) as the data points corresponding to the $\bar{R}_H$ of pullulans using either 0.1 M KOH[23] or pure water[19] as solvent belong to the same master curve.

A second matter of discussion deals with the differences in the macromolecular features deduced from SEC−MALLS and SANS experiments.

A method already used[6] allowing the extraction of the persistence length from $\bar{R}_{Gw}$ and $\bar{M}_w$ data is detailed below. The basis for this method is first to introduce the definition of the characteristic ratio C_∞

$$C_\infty = \lim_{n \to \infty} \frac{\langle r^2 \rangle_0}{nl^2} \tag{15}$$

where $\langle r^2 \rangle_0$ is the mean-square end-to-end distance of the unperturbed coil, l is the average projection length of a monomer on the segment axis, and n is the degree of polymerization of the chain.

When a random coil is considered, $\langle r^2 \rangle_0$ is proportional to the mean-square radius of gyration through the relation

$$\langle r^2 \rangle_0 = 6\bar{R}_{G0}{}^2 \tag{16}$$

where $\bar{R}_{G0}$ is the root-mean-square radius of gyration obtained under the Θ conditions.

Then for a polymer possessing a distribution of molecular mass and reaching a sufficient mean average degree of polymerization $\bar{n}_w$

$$\bar{n}_w = \bar{M}_w/M_0 \tag{17}$$

where M_0 is the molar mass of the monomer unit, for an anhydroglucose residue = 162 g·mol^{-1}, and $\bar{M}_w$ is the weight-average molar mass.

The characteristic ratio can then be successively written as

$$C_\infty = \frac{6\bar{R}_{G0w}{}^2}{\bar{n}_w l^2} = \frac{6\bar{R}_{G0w}{}^2 M_0}{\bar{M}_w l^2} = \frac{\bar{R}_{G0w}{}^2 6M_0}{\bar{M}_w \quad l^2} \tag{18}$$

Generally chain expansion has to be taken into account because for most studies rather good solvent conditions are chosen. So it is not R_{G0w} (which is the ideal dimension of the chain in an unperturbed condition, the so-called Θ condition obtained at a given temperature called the Θ temperature) that is experimentally obtained but R_{Gw}. The long-range excluded-volume effect is expressed by the semiempirical expansion factor α with

$$\bar{R}_{Gw}{}^2 = \alpha^2 \bar{R}_{G0w}{}^2 \tag{19}$$

By combining eqs 18 and 19, we obtain

$$\frac{\bar{R}_{Gw}{}^2}{\bar{M}_w} = \alpha^2 \frac{\bar{R}_{G0w}{}^2}{\bar{M}_w} = \alpha^2 \frac{C_\infty l^2}{6M_0} \tag{20}$$

α^2 is a function of the excluded parameter z, defined by

$$z = \left(\frac{3}{2\pi}\right)^{3/2} B\left(\lim_{M\to\infty} \frac{\langle r^2\rangle_0}{M}\right)^{-3/2} \bar{M}_w{}^{1/2} \tag{21}$$

with $B = \beta/M_s{}^2$, where M_s is the molar mass of the segment and β the effective volume of the segment excluded to one segment by the presence of another. The parameter B is positive in good solvents and equals zero at the Θ-temperature.

According to perturbation theories,[24] for small z in the close vicinity of the Θ-temperature where $\alpha^2 \to 1$

$$\alpha^2 = 1 + \sum_i a_i z^i \tag{22}$$

which becomes when considering only the first-order relationship

$$\alpha^2 = 1 + \frac{134}{105} z \tag{23}$$

De Gennes[17] has established the polymer−magnet analogy, which enables one to write the asymptotic behavior for large z

$$\alpha^2(z) = Az^{2(2\nu-1)}(1 + bz^{-2\Delta} + ...) \tag{24}$$

where "the critical exponents" ν and Δ are theoretically well-determined universal constants. The constants A and b are amplitudes of the leading power law and correction-to-scaling terms.

So for small z, the square expansion factor α^2 may be expressed as a function of $M_w{}^{0.5}$ by combining eqs 21 and 23

$$\alpha^2 = 1 + \left[\frac{134}{105}\left(\frac{3}{2\pi}\right)^{3/2} B\left(\lim_{M\to\infty} \frac{< r^2 >_0}{M}\right)^{-3/2}\right] \bar{M}_w{}^{1/2} \tag{25}$$

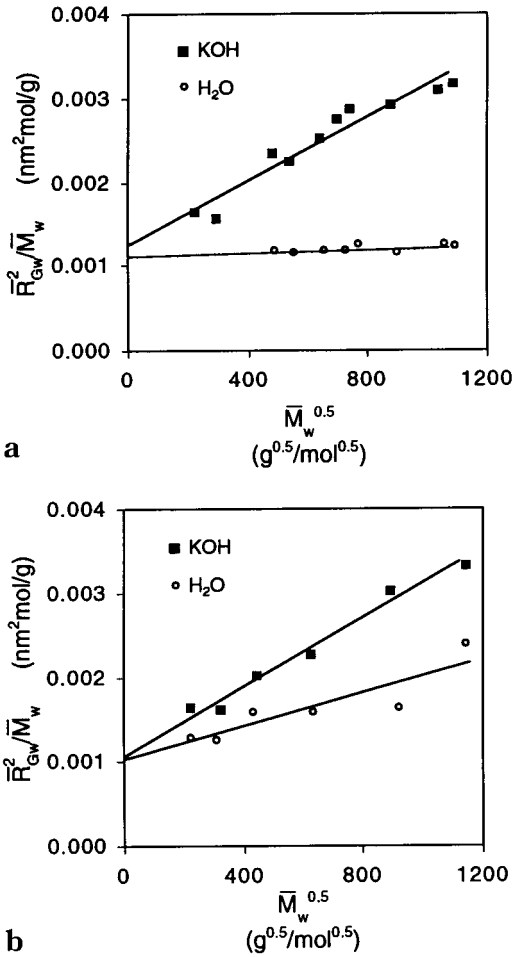

Figure 9. Plots of $\bar{R}_G{}^2/\bar{M}_w$ vs $\bar{M}_w{}^{0.5}$ using H_2O and 0.1 M KOH as solvent (a, top) of amylose fractions and (b, bottom) of pullulan fractions.

which can be written under the simplified form

$$\alpha^2 = 1 + c'\bar{M}_w{}^{1/2} \tag{26}$$

Then eq 20 can be written

$$\frac{\bar{R}_{Gw}{}^2}{\bar{M}_w} = \frac{C_\infty l^2}{6M_0}(1 + c'\,\bar{M}_w{}^{1/2}) \tag{27}$$

So the intercept with the ordinates of the variation of $\bar{R}_{Gw}{}^2/\bar{M}_w$ with $\bar{M}_w{}^{0.5}$ gives $C_\infty l^2/6M_0$ and consequently the value of the characteristic ratio C_∞. This relationship has been plotted (Figure 9a) for amylose in both solvents. The extrapolation line in KOH has a positive slope whereas in water $\bar{R}_{Gw}{}^2/\bar{M}_w$ is nearly independent of $M_w{}^{0.5}$. This result indicates that (i) excluded volume effect is more predominant in KOH than in water and that, (ii) in water, amylose is not far from the Θ conditions where no exclusion volume effects take part. That also means that c' is a constant, independent of $\bar{M}_w$ and that it seems possible to use eq 27 to find the C_∞ value even under good solvent conditions, i.e., for a large z value.

By using a monomeric length of 0.425 nm,[25] the extrapolation to zero ordinate gives a characteristic ratio C_∞ of 6.0 ± 0.3 and 6.7 ± 0.7 considering H_2O and KOH 0.1 M, respectively, as solvent. These values are in complete agreement with previous results.[15,26,27]

Then the persistence length is deduced from C_∞ using the relationship valid for a linear Gaussian chain:[28]

$$C_\infty = \frac{2a}{l} - 1 \tag{28}$$

By using eq 28, values of the persistence length are $a = 1.5 \pm 0.1$ nm and $a = 1.6 \pm 0.2$ nm considering H_2O and KOH 0.1 M, respectively, as solvent.

If the same procedure is applied to pullulan data (Figure 9b), by using a monomeric length of 0.479 nm,[29] then the values of the characteristic ratio C_∞ are slightly lower: 4.3 ± 0.8 and 4.6 ± 0.5 considering H_2O and KOH 0.1 M, respectively, as solvent. The value of $C_\infty = 4.3$ obtained in water is the same as the one obtained in aqueous solution at 25 °C by others.[29,30]

Then using eq 13, the values of the persistence length are $a = 1.3 \pm 0.2$ nm and $a = 1.3 \pm 0.1$ nm considering H_2O and KOH 0.1 M, respectively, as solvent. The values of the relative characteristic ratios and persistence lengths of amylose and pullulan show that aqueous pullulan and aqueous amylose have essentially the same chain dimensions by this measure.

By SANS the persistence lengths obtained are significantly higher than the value obtained by SEC−MALLS. Using D_2O, a is found to increase slightly from 1.9 to 3.2 nm as the molar mass decreases from 8×10^5 down to 3×10^5 g·mol^{-1} which could be explained by an increase in helicity as the molar mass decreases, i.e., as the dissolving gap approaches. The value of 4.2 nm obtained in KOD looks obscure to us unless a complex formation leads to an increase in chain rigidity.

It is also possible to extract a molar mass per unit length, M_L, from the SEC−MALLS results by fitting the experimental $\bar{R}_G$ vs $\bar{M}_w$ data to the theoretical equation established for semiflexible chains[31]

$$\bar{R}_G{}^2 = a^2/3((L/a - 1) + \exp(-L/a)) \tag{29}$$

where L, the total contour length, is equal to $L = M/M_L$.

By using the value of the persistence length obtained above with H_2O as solvent, $a = 1.5$ nm, the value of the molar mass per unit length is $M_L = 410$ g/mol/nm. That experimental value is very close to the limit value calculated for the most stretched polymorph with $h = 0.4$ nm/monomer and $M_L = 400$ g/mol/nm and far from that evaluated[32] for the more compact helix with $h = 0.1$ nm/monomer for the eight-residue V helix and $M_L = 1620$ g/mol/nm. The quantity h represents the contour length of the chain per monomer unit and is defined by

$$h = M_0/M_L \tag{30}$$

The M_L values obtained by SANS using KOD as a solvent are rather comparable to the SEC−MALLS value using H_2O with an average value of 458 ± 28 g/mol/nm. Surprisingly, the values of M_L obtained by SANS using D_2O as solvent increase from 440 to 570 g/mol/nm as the molar mass decreases from 8×10^5 down to 3×10^5 g·mol^{-1}. That probably means that amylose fractions are more stable using KOD against D_2O as solvent and furthermore that there is a preferential interchain aggregation as the molar mass decreases considering the results in D_2O. That can also explain the higher $\bar{R}_G$ values obtained in D_2O by fitting the SANS intensity curves when compared to the $\bar{R}_G$ values obtained by SEC−MALLS in H_2O. The decrease in solvent quality when D_2O is used instead of H_2O is also emphasized by the simple fact that it is necessary to keep the amylose solutions dissolved in D_2O at least at a temperature of 40 °C to avoid precipitation whereas amylose solutions are stable down to 25 °C if H_2O is used. It finally means that D solvents are suitable for studying α-glucan solutions but physicochemical properties of the system polymer−solvent can present significant changes as compared to classical aqueous solvents.

The last point of this discussion concerns the fact that the macromolecular features obtained by analyzing either the SEC−MALLS or the SANS data characterize a highly flexible polymer in solution. How could amylose adopt such a flexible conformation since the local geometry structure of amylose essentially forces the chain to adopt a pseudohelical trajectory?[25] To explain this let us consider the global relaxed potential energy surface of maltose (Figure 5 of ref 33) more commonly called the (Φ,Ψ) map (where Φ and Ψ are two torsional angles defined as Φ = O(5)−C(1)−O(1)−C(4′) and Ψ = C(1)−O(1)−C(4′)−C(5′)) and the corresponding (n,h) maps of the α(1→4) glucan chain (Figure 4c of ref 34), where the iso-n and iso-h are shown. Here n and h are the two parameters used customarily to describe the helical character of a polymer chain, n being the number of residues per turn of the helix, and h being the translation of the corresponding residue along the axis of the helix. We can conclude after superposition of those two maps that there is a main area with the more stable conformers A, B, C, and D, obtained for (Φ,Ψ) ∼ (60,−150) which corresponds to h equals 0 with a large variation (negative values of h corresponding to the left-handed helix and positive values to the right-handed helix) and n values of 6 ± 1. In this area, amylose behaves as a rather compact helix. In that case, our conformational exponent ν should exhibit a more pronounced semiflexible character with a higher value than 0.5−0.6. What could explain our experimental ν value is the presence of another stable area with conformers E and F, obtained for (Φ,Ψ) ∼ (90,60), which corresponds to a maximum value of h and to $n \sim 2$. This conformation corresponds to a maximum elongation which is less probable but which can occur statistically all along the α(1→4) chain conferring to the amylose chain a global high flexible character as confirmed by our experimental ν exponent.

Acknowledgment. The authors gratefully acknowledge Catherine Hillion, Frédérique Martin, and Roselyne Desirest, for their successive excellent technical assistance provided for the amylose synthesis and the SEC−MALLS experiments. A special thanks is given to François Boué (Laboratoire Léon Brillouin, C.E.-Saclay, France) and Denis Renard (INRA-Nantes, in a postdoctoral position at the LLB during this period) for their help during the SANS experiments and to Vinh Huu Tran (INRA-Nantes) for his clear explanation about the helical conformation of amylose.

References and Notes

(1) (a) *Food polysaccharides and their applications*; Stephen, A. M. Ed.; Marcel Dekker: New York, 1995. (b) Doublier, J. L.; Cuvelier, G. Gums and hydocolloids: functional aspects. In *Carbohydrates in food*; Eliasson, A.-C., Ed.; Marcel Dekker: New York, 1996.
(2) Wyatt, P. J.; Papazian, L. A. *LC GC* **1993**, *11*, 862.
(3) Shortt, D. W. *J. Chromatogr. A* **1994**, *686*, 11.
(4) Roger, P.; Colonna, P. *Carbohydr. Polym.* **1993**, *21*, 83.

(5) Roger, P.; Tran, V.; Lesec, J.; Colonna, P. *J. Cereal Sci.* **1996**, *24*, 247.
(6) Roger, P.; Colonna, P. *Carbohydr. Res.* **1992**, *227*, 73.
(7) Husemann, E.; Pfannemüller, B. *Makromol. Chem.* **1961**, *49*, 214.
(8) Pfannemüller, B. *Starch/Stärke* **1968**, *20*, 351.
(9) Gidley, M. J.; Bulpin, P. V. *Macromolecules* **1989**, *22*, 341.
(10) Lowry, O. H.; Rosebrough, N. J.; Farr, A. L.; Randall, S. J. *J. Biol. Chem.* **1951**, *193*, 265.
(11) Lowry, O. H.; Lopez, J. A. *J. Biol. Chem.* **1946**, *162*, 421.
(12) Planchot, V.; Colonna, P.; Saulnier, L. In *Guide pratique d'analyses dans les industries des céréales*; Godon, B., Loisel, W., Eds., Lavoisier: Paris, 1996; p 350.
(13) Paschall, E. F.; Foster, J. F. *J. Polym. Sci.* **1952**, *9*, 85.
(14) Kirste, R. G.; Oberthür, R. C. In *Small-angle X-ray sacttering*; Glatter, O., Kratky, O., Eds., Academic Press: Paris, 1982; p 387.
(15) Nakanishi, Y.; Norisuye, T.; Teramoto, A.; Kitamura, S. *Macromolecules* **1993**, *26*, 4220.
(16) Flory, P. J. *Principles of Polymer Chemistry*; Cornell University Press: Ithaca, NY, 1953.
(17) de Gennes, P. G. *Scaling concept in polymer chemistry*; Cornell University Press: Ithaca, NY, 1979; pp 29−53.
(18) Le Guillou, J. C.; Zinn-Justin, J. *Phys. Rev. Lett.* **1977**, 39, 95.
(19) Kato, T.; Katsuki, T.; Takahashi, A. *Macromolecules* **1984**, *17*, 1726.
(20) Burchard, W. *Macromol. Chem.* **1963**, *59*, 16.
(21) Takeda, Y.; Shirasaka, K.; Hizukuri, S. *Carbohydr. Res.* **1984**, *132*, 83.
(22) Burchard, W.; Schmidt, M.; Stockmayer, W. H. *Macromolecules* **1980**, *13*, 1265.
(23) Roger, P. Ph.D. Thesis, Nantes, 1993.
(24) Yamakawa, H. *Modern Theory of Polymer Solution*; Harper and Row: New York, 1971.
(25) Brant, D. A.; Burton, B. A. *Solution Properties of Polysaccharides*; American Chemical Society, Washington, DC, 1981; pp 81−99.
(26) Banks, W.; Greenwood, C. T. *Starch & its Components*; Edinburgh University Press: Edinburgh, Scotland, 1975.
(27) Ring, S. G.; I'Anson, K. J.; Morris, V. J. *Macromolecules* **1985**, *18*, 182.
(28) Flory, P. J. *Statistical mechanics of chain molecules*; Interscience: New York, 1969; p 111.
(29) Buliga, G. S.; Brant D. A. *Int. J. Biol. Macromol.* **1987,** *9*, 71.
(30) Kato, T.; Okamoto, T.; Tokuya, T.; Takahashi, A. *Biopolymers* **1982**, *21*, 1623.
(31) Benoît, H.; Doty, P. *J. Phys. Chem.* **1953**, *53*, 3, 958.
(32) French, A. D.; Murphy V. G. *Polymer* **1977**, *18*, 489.
(33) Tran, V.; Buléon A.; Imberty, A.; Perez, S. *Biopolymers* **1989** *28*, 679.
(34) Gagnaire, D.; Perez, S., Tran, V. *Carbohydr. Res.* **1980**, *78*, 89.

MA991302S